Stability of Dark Solitons in Three Dimensional Dipolar Bose-Einstein Condensates

R. Nath,[1] P. Pedri,[2,3] and L. Santos[1]

[1]*Institut für Theoretische Physik, Leibniz Universität Hannover, Appelstr. 2, D-30167, Hannover, Germany*
[2]*Laboratoire de Physique Théorique et Modèles Statistiques, Universit Paris Sud, 91405 Orsay Cedex, France*
[3]*Laboratoire de Physique Théorique de la Matière Condensée, Université Pierre at Marie Curie, case courier 121, 4 place Jussieu, 75252 Paris Cedex, France*

(Received 22 December 2007; published 19 November 2008)

The dynamical stability of dark solitons in dipolar Bose-Einstein condensates is studied. For standard short-range interacting condensates, dark solitons are unstable against transverse excitations in two and three dimensions. On the contrary, due to its nonlocal character, the dipolar interaction allows for stable 3D stationary dark solitons, opening a qualitatively novel scenario in nonlinear atom optics. We discuss in detail the conditions to achieve this stability, which demand the use of an additional optical lattice, and the stability regimes.

DOI: 10.1103/PhysRevLett.101.210402 PACS numbers: 03.75.Lm, 05.30.Jp, 05.45.Yv

The physics of Bose-Einstein condensates (BECs) is, due to the interatomic interactions, inherently nonlinear, closely resembling the physics of other nonlinear systems, and, in particular, nonlinear optics. Nonlinear atom optics [1] has indeed attracted a major attention in the last years, including phenomena like four-wave mixing [2] and condensate collapse [3]. One of the major consequences of nonlinearity is the possibility of achieving solitons in quasi-1D BECs. Bright solitons have been reported in BECs with s-wave scattering length, $a < 0$ (equivalent of self-focusing nonlinearity) [4]. Dark solitons (DSs) have been realized as well as in BECs with $a > 0$ (self-defocusing nonlinearity) [5]. In addition, optical lattices have allowed for the observation of gap solitons [6].

At zero temperatures, soliton stability crucially depends on quasi-one dimensionality, which for BECs demands a sufficiently strong transversal confinement [7]. For the case of DSs, if the transversal size of the system becomes comparable to the width of the DS ($\sim$ healing length), then the DS becomes dynamically unstable. This dynamical instability (so-called *snake instability*, see Fig. 1) has been previously studied in the context of nonlinear optics [8]. In the context of BEC, it has been shown that this instability leads to a strong bending of the nodal plane, which breaks down into vortex rings and sound excitations [9], as experimentally observed in Ref. [10]. In the presence of dissipation, thermodynamical instabilities may be important [11], and in other cases nonlinear instabilities may completely change the dynamics [12].

Nonlinear phenomena constitute an excellent example of the crucial role played by interactions in quantum gases. Until recently, typical experiments involved particles interacting dominantly via short-range isotropic potentials, which, due to the very low energies involved, are determined by the corresponding s-wave scattering length. However, recent experiments on cold molecules [13], atoms with large magnetic moment [14], spinor BEC [15], and alkali-metal BEC in optical lattices [16], open a fascinating new research area, namely, that of dipolar gases, for which the dipole-dipole interaction (DDI) plays a significant role. The DDI is long-range and anisotropic (partially attractive), and leads to fundamentally new physics in ultra cold gases [17]. Time-of-flight experiments in Cr BEC have allowed for the first observation of DDI effects in cold gases [18], which have been remarkably enhanced by means of Feshbach resonances [19].

Dipolar gases present a rich nonlinear physics, since the DDI leads to nonlocal nonlinearity, similar as that encountered in plasmas [20], nematic liquid crystals [21], thermo-optical materials [22], and photo-refractive crystals [23]. Nonlocality leads to a wealth of novel phenomena in nonlinear physics, as the modification of modulation instability [24], the change of the soliton interaction [25], and the stabilization of azimuthons [26]. Particularly interesting is the possibility of stabilization of localized waves in cubic nonlinear materials with a symmetric nonlocal nonlinear response [27]. Multidimensional solitons have been experimentally observed in nematic liquid crystals [28] and in photo-refractive screening solitons [29]. Recently, we showed that 2D bright inelastic solitons may be generated in dipolar BEC [30]. Other ways of stabilizing multidimensional solitons, not involving DDI, have been recently proposed [31].

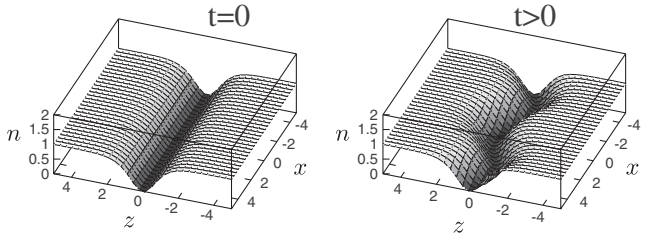

FIG. 1. Density plot of the Snake Instability: The Dark Soliton at $t = 0$ starts to oscillate and eventually breaks.

In this Letter, we show that the long-range character of the DDI may have striking consequences for the stability of DSs in dipolar BECs. Contrary to usual BECs, for which, as mentioned above, DSs become unstable when departing from the 1D condition, the DDI may stabilize DSs in a 3D environment. This stabilization is purely due to the long-range and anisotropic characters of the DDI. We study in detail the conditions for this stabilization, and the stabilization regimes.

In the following, we consider a dipolar BEC of particles with mass m and electric dipole d (the results are equally valid for magnetic dipoles) oriented in the z-direction by a sufficiently large external field, and that hence interact via a dipole-dipole potential: $V_d(\vec{r}) = \alpha d^2[1 - 3\cos^2(\theta)]/r^3$, where θ is the angle formed by the vector joining the interacting particles and the dipole interaction. The coefficient α can be tuned within the range $-1/2 \leq \alpha \leq 1$ by rotating the external field that orients the dipoles much faster than any other relevant time scale in the system [32]. At sufficiently low temperatures, the physics of the dipolar BEC is provided by the nonlocal nonlinear Schrödinger equation (NLSE):

$$i\hbar\frac{\partial}{\partial t}\Psi(\vec{r},t) = \Big[-\frac{\hbar^2}{2m}\nabla^2 + V_{\rm ol}(x,y) + g|\Psi(\vec{r},t)|^2 + \int d\vec{r}\,' V_d(\vec{r}-\vec{r}\,')|\Psi(\vec{r}\,',t)|^2\Big]\Psi(\vec{r},t), \quad (1)$$

where $g = 4\pi\hbar^2 a/m$, with a the s-wave scattering length and m the particle mass. For reasons that will become clear below, the BEC is assumed to be in a 2D optical lattice, $V_{\rm ol}(x,y) = sE_R[\sin^2(q_l x) + \sin^2(q_l y)]$, where $E_R = \hbar^2 q_l^2/2m$ is the recoil energy, q_l is the laser wave vector, and s is a dimensionless parameter providing the lattice depth. In the tight-binding regime (i.e., for a sufficiently strong lattice but still maintaining coherence), we may write $\Psi(\vec{r},t) = \Sigma_{i,j} w_{ij}(x,y)\psi_{i,j}(z,t)$, where $w_{ij}(x,y)$ is the Wannier function associated to the lowest energy band and the site located at (bi, bj), with $b = \pi/q_l$. Substituting this ansatz in Eq. (1), we obtain a discrete NLSE [33]. We may then return to a continuous equation, where the lattice is taken into account in an effective mass along the lattice directions and in the renormalization of the coupling constant [34].

$$i\hbar\frac{\partial}{\partial t}\Psi(\vec{r},t) = \Big[-\frac{\hbar^2}{2m^*}\nabla_{\vec{\rho}}^2 - \frac{\hbar^2}{2m}\frac{\partial^2}{\partial z^2} + \tilde{g}|\Psi(\vec{r},t)|^2 + \int d\vec{r}\,' V_d(\vec{r}-\vec{r}\,')|\Psi(\vec{r}\,',t)|^2\Big]\Psi(\vec{r},t), \quad (2)$$

where $\tilde{g} = b^2 g \int w(x,y)^4 dxdy + g_d C$ [35], with $g_d = \alpha 8\pi d^2/3$, $m^* = \hbar^2/2b^2 J$ is the effective mass, and $J = \int dxdy w_{ij}(x,y)[-(\hbar^2/2m)\nabla_{\vec{\rho}}^2 + V_{\rm ol}(x,y)]w_{i'j'}(x,y)$, for neighboring sites (i, j) and (i', j'). The validity of Eq. (2) is limited to radial momenta $k_\rho \ll 2\pi/b$, in which one can ignore the discreteness of lattice. In addition, the single-band model breaks down if the gap to the second band becomes comparable to other energy scales ($m/m^* \to 1$). In the following, we use the dimensionless parameter $\beta = g_d/\tilde{g}$ that characterizes the strength of the DDI compared to the short-range interaction.

Because of its partially attractive character, the stability of a dipolar BEC is a matter of obvious concern [17]. Bogoliubov analysis of an homogeneous dipolar BEC gives the dispersion relation for quasiparticles is of the form $\epsilon(\vec{k}) = \{E_{\rm kin}(\vec{k})[E_{\rm kin}(\vec{k}) + E_{\rm int}(\vec{k})]\}^{1/2}$, where $E_{\rm kin} = \hbar^2 k_\rho^2/2m^* + \hbar^2 k_z^2/2m$ is the kinetic energy, and $E_{\rm int} = 2[g + \tilde{V}_d(\vec{k})]n_0$ is the interaction energy, which includes both short-range and dipolar parts. Note that $\tilde{V}_d(\vec{k}) = g_d[3k_z^2/|\vec{k}|^2 - 1]/2$ (Fourier transform of the DDI) may be positive or negative, and hence for low momenta ($\vec{k} \to \vec{0}$), the dynamical phonon instability is prevented if $-1 < \beta < 2$. If $g_d > 0$, phonons with $\vec{k}$ lying on the xy plane are unstable if $\beta > 2$, while for $g_d < 0$ phonons with $\vec{k}$ along z are unstable if $\beta < -1$ [36].

In this Letter, we are concerned about the stability of a DS in a 3D dipolar BEC. We assume that the DS lies on the xy plane; hence, the solution can be written as $\Psi_0(\vec{r},t) = \psi_0(z)\exp[-i\mu t/\hbar]$, where μ is the chemical potential. Introducing this expression into Eq. (1), we obtain a 1D NLSE in z of the form

$$\mu\psi_0(z) = \Big[-\frac{\hbar^2}{2m}\frac{\partial^2}{\partial z^2} + \bar{g}|\psi_0(z)|^2\Big]\psi_0(z). \quad (3)$$

Since ψ_0 is independent of x and y, in Eq. (3) the DDI just regularizes the value of the local coupling constant $\bar{g} = \tilde{g} + g_d$. Equation (3) allows for a simple solution describing a DS, $\psi_0 = \sqrt{n_0}\tanh(z/\zeta)$, where $\zeta = \hbar/\sqrt{m\bar{g}n_0}$ is the corresponding healing length and n_0 is the bulk density.

We study the DS stability by means of a Bogoliubov analysis, considering a transversal perturbation in the nodal plane, $\Psi(\vec{r},t) = \Psi_0(\vec{r},t) + \chi(\vec{r},t)\exp(-i\mu t/\hbar)$, where $\chi(\vec{r},t) = u(z)\exp[i(\vec{q}\cdot\vec{\rho} - \epsilon t/\hbar)] + v(z)\exp[-i(\vec{q}\cdot\vec{\rho} - \epsilon t/\hbar)]$, where q is the momentum of the transverse modes with energy ϵ. Introducing this ansatz into (1) and linearizing in χ, one obtains the Bogoliubov-de Gennes (BdG) equations for the excitation energies ϵ and the corresponding eigenfunctions $f_\pm = u \pm v$:

$$\epsilon f_-(z) = \Big[-\frac{\hbar^2}{2m}\Big(\frac{\partial^2}{\partial z^2} - \frac{m}{m^*}q^2\Big) - \mu + 3\bar{g}\psi_0(z)^2\Big] \times f_+(z) - \frac{3}{2}g_d q\psi_0(z)\int_{-\infty}^{\infty} dz'\exp(-q|z - z'|)\psi_0(z')f_+(z'), \quad (4)$$

$$\epsilon f_+(z) = \Big[-\frac{\hbar^2}{2m}\Big(\frac{\partial^2}{\partial z^2} - \frac{m}{m^*}q^2\Big) - \mu + \bar{g}\psi_0(z)^2\Big]f_-(z). \quad (5)$$

The lowest eigenvalue $\epsilon(q)$ for each q provides the dispersion law. Note that the DDI has two main effects: (i) it leads

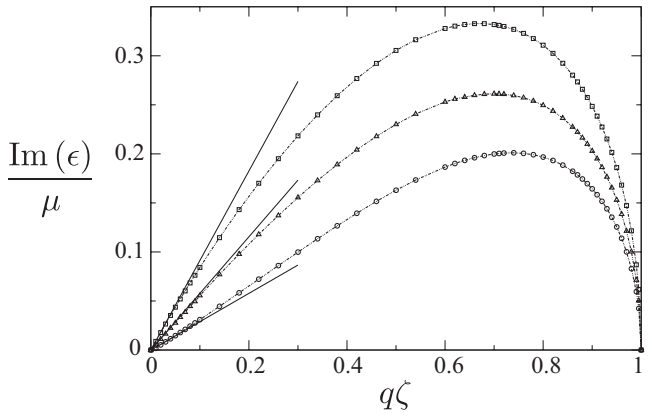

FIG. 2. Numerical results for the imaginary part of the excitation energies of a DS for $m/m^* = 1$, and $\beta = 0$ (triangles), -0.5 (squares), and 1 (circles). Solid lines correspond to the analytical result for low momenta.

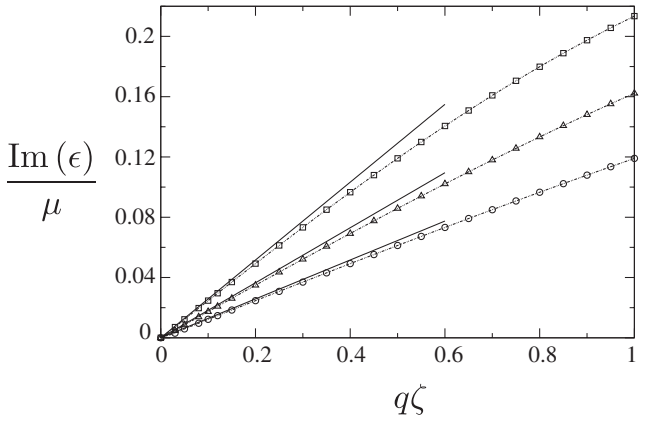

FIG. 3. Numerical results for the imaginary part of the excitation energies of a DS for $\beta = 0$, and $m/m^* = 0.2$ (squares), 0.1 (triangles), and 0.05 (circles). Solid lines correspond to the analytical result for low momenta.

to a regularized $\bar{g}$, and (ii) it introduces a qualitatively new term in the second line of Eq. (4). Whereas the first effect leads to a quantitative modification of the DS width, the second effect is a purely dipole-induced nonlocal effect, which, as we show below, may lead to remarkable consequences for the DS stability.

When $\beta = 0$ (no DDI) and $m/m^* = 1$ (no lattice), we recover the BdG equations obtained in the case of standard short-range interacting BECs [7]. It has been shown that in that case the dispersion law $\epsilon(q)$ is purely imaginary for $q\zeta < 1$ (Fig. 2). Hence, DSs in homogeneous 3D short-range interacting BECs are dynamically unstable against transverse modulations. Because of this instability, the nodal plane acquires a characteristic snakelike bending. This so-called *snake instability* (see Fig. 1) has been experimentally observed in nonlinear optics [8] and recently in the context of BEC [10]. In the latter case, the bending results in the decay of a DS into vortex rings and sound excitations [9]. In the presence of a 2D lattice, we found by means of the model developed in Ref. [34] that the DS remains dynamically unstable (see Fig. 3).

In the presence of DDI ($\beta \neq 0$) but without lattice ($m/m^* = 1$), the transverse instability persists since $\epsilon(q)$ remains imaginary for $q\zeta < 1$. For $\beta > 0$ ($\beta < 0$), $|\epsilon(q)|$ decreases (increases) when $|\beta|$ grows (Fig. 2). The situation can change dramatically in the presence of both the DDI and a lattice. Surprisingly, for sufficiently large dipoles and small m/m^*, $\epsilon(q)$ becomes real and hence the DS becomes dynamically stable (see Fig. 4). This remarkable fact can be understood by analyzing the surface tension of the nodal plane. First, we notice that for low momenta $\epsilon(q)$ is always linear in q, suggesting the idea that for low momenta, the nodal plane may be described by an elastic model with Lagrangian density, $\mathcal{L}(\partial\phi/\partial t, \vec{\nabla}\phi) = (M/2)(\partial\phi/\partial t)^2 - (\sigma/2)|\vec{\nabla}\phi|^2$, where ϕ is the displacement field of the nodal plane from the ground state, M is the mass per unit area, and σ plays the role of a surface tension. By expanding the energy of a moving soliton up to second order in the velocity, we obtain the soliton mass $M = -4\hbar n_0/c$, where $c = \sqrt{\bar{g}n_0/m}$ is the sound velocity. Note that $M < 0$. We calculate σ by inserting a variational ansatz $\Psi_{\text{var}}(\vec{r}) = \sqrt{n_0}\tanh\{[z - \sqrt{2}\alpha\cos(qx)]/\zeta\}$ (a transverse modulation of the nodal plane with amplitude α and momentum q) in the energy functional and expanding up to second order in α and q:

$$\sigma = 4n_0\hbar^2/3\zeta m^* - 2g_d n_0^2\zeta. \tag{6}$$

This expression can be considered as one of the main results of this Letter. The eigenmodes, $\epsilon^2/\hbar^2 = \omega^2 = (\sigma/M)q^2$, which provide the low-energy linear excitations of the DS, can be either purely real or purely imaginary, crucially depending on the sign of σ/M. In the absence of DDI ($\beta = 0$), σ is always positive, the modes are purely imaginary, and hence the DS shows snake instability for any value of m/m^* (4). The stabilization hence is a characteristic feature introduced by the DDI. Note that for $\beta = 0$ and $m/m^* = 1$, our result coincides with the one found in

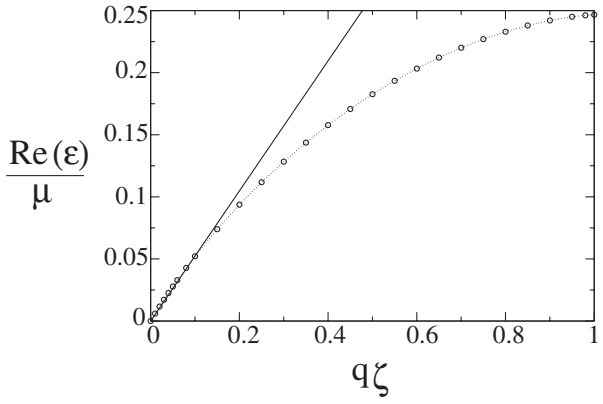

FIG. 4. Real part of the excitation energies of a DS for $m/m^* = 0.1$ and $\beta = 1.6$. Solid line corresponds to the analytical result for low momenta while empty circles correspond to numerical results.

Ref. [7]. In the absence of an additional optical lattice, the dynamical instability of the DS at low q disappears for $\beta > 2$, i.e., for situations for which the homogeneous dipolar BEC as a whole is itself, as commented above, unstable against local collapses. Increasing the depth of the lattice potential reduces the role of the kinetic energy term $(m/m^*)q^2$ in Eqs. (4) and (5) [or equivalently reduces the first term in Eq. (6)] and hence enhances the role of DDI. A sufficiently large DDI or small $m/m^* < (m/m^*)_{\rm cr} = 3\beta/2(1+\beta)$ leads to stable low-energy ($q \to 0$) linear excitations. We have confirmed that this analytical result coincides with our results obtained from BdG Eqs. (4) and (5). When m/m^* decreases further or β grows, a wider regime of momenta up to $q\sqrt{m/m^*}\zeta \sim 1$ is stabilized (Fig. 4). Indeed, direct numerical simulations of Eq. (2) show that the dark nodal plane becomes completely stable against snake instability, whereas under the same conditions, the DS is unstable in absence of DDI. Instabilities may appear for momenta $q\sqrt{m/m^*}\zeta \sim 1$, but this large-momentum instability is typically irrelevant, since for sufficiently small m/m^* it concerns momenta much larger than the lattice momentum. Although our effective mass theory breaks down for such momenta, it becomes clear that such high momentum instabilities are physically prevented by the zero point oscillations at each lattice site [37].

Summarizing, contrary to short-range interacting BECs, where snake instability is just prevented by a sufficiently strong transverse confinement, dipolar BECs allow for stable dark solitons of arbitrarily large transversal sizes (dissipation would eventually lead to thermodynamical instability [11] whose detailed analysis, as well as that of quantum instabilities [38], demands a separate work). We have obtained the stability conditions, which demand a sufficiently large dipole and a sufficiently deep optical lattice in the nodal plane. We stress that the stabilization of nodal planes against snake instability is purely linked to the long-range nature of the DDI, opening a qualitatively new scenario in nonlinear atom optics.

We acknowledge fruitful discussions with L. P. Pitaevskii, L. Pricoupenko, and G. V. Shlyapnikov. This work was supported by the DFG (SFB-TR21, SFB407, SPP1116), by the Ministère de la Recherche (Grant ACI Nanoscience 201), by the ANR (Grants Nos. NT05-2_42103 and 05-Nano-008-02), and by the IFRAF Institute. LPTMC is UMR 7600 of CNRS.

[1] P. Meystre, *Atom Optics* (Springer Verlag, New York, 2001).
[2] L. Deng *et al.*, Nature (London) **398**, 218 (1999).
[3] E. A. Donley *et al.*, Nature (London) **412**, 295 (2001).
[4] K. E. Strecker *et al.*, Nature (London) **417**, 150 (2002); L. Khaykovich *et al.*, Science **296**, 1290 (2002).
[5] S. Burger *et al.*, Phys. Rev. Lett. **83**, 5198 (1999); J. Denschlag *et al.*, Science **287**, 97 (2000).
[6] B. Eiermann *et al.*, Phys. Rev. Lett. **92**, 230401 (2004).
[7] A. E. Muryshev *et al.*, Phys. Rev. A **60**, R2665 (1999).
[8] V. Tikhonenko *et al.*, Opt. Lett. **21**, 1129 (1996); A. V. Mamaev *et al.*, Phys. Rev. Lett. **76**, 2262 (1996).
[9] D. L. Feder *et al.*, Phys. Rev. A **62**, 053606 (2000).
[10] B. P. Anderson *et al.*, Phys. Rev. Lett. **86**, 2926 (2001).
[11] A. Muryshev *et al.*, Phys. Rev. Lett. **89**, 110401 (2002).
[12] A. P. Itin and S. Watanabe, Phys. Rev. Lett. **99**, 223903 (2007).
[13] S. Ospelkaus *et al.*, Nature Phys. **4**, 622 (2008).
[14] A. Griesmaier *et al.*, Phys. Rev. Lett. **94**, 160401 (2005); Q. Beaufils *et al.*, Phys. Rev. A **77**, 061601(R) (2008).
[15] M. Vengalattore *et al.*, Phys. Rev. Lett. **100**, 170403 (2008).
[16] M. Fattori *et al.*, arXiv:0808.1506.
[17] S. Yi and L. You, Phys. Rev. A **61**, 041604(R) (2000); K. Góral, K. Rzążewski, and T. Pfau, Phys. Rev. A **61**, 051601(R) (2000); L. Santos *et al.*, Phys. Rev. Lett. **85**, 1791 (2000); L. Santos, G. V. Shlyapnikov, and M. Lewenstein, Phys. Rev. Lett. **90**, 250403 (2003); S. Giovanazzi and D. H. J. O'Dell, Eur. Phys. J. D **31**, 439 (2004); M. A. Baranov *et al.*, Phys. Rev. Lett. **92**, 250403 (2004); K. Góral *et al.*, Phys. Rev. Lett. **88**, 170406 (2002); E. H. Rezayi, N. Read, and N. R. Cooper, Phys. Rev. Lett. **95**, 160404 (2005).
[18] J. Stuhler *et al.*, Phys. Rev. Lett. **95**, 150406 (2005).
[19] Th. Lahaye *et al.*, Nature (London) **448**, 672 (2007).
[20] A. G. Litvak *et al.*, Sov. J. Plasma Phys. **1**, 31 (1975).
[21] M. Peccianti *et al.*, Nature (London) **432**, 733 (2004).
[22] C. Rotschild *et al.*, Phys. Rev. Lett. **95**, 213904 (2005).
[23] G. C. Duree *et al.*, Phys. Rev. Lett. **71**, 533 (1993).
[24] W. Królikowski *et al.*, Phys. Rev. E **64**, 016612 (2001).
[25] N. I. Nikolov *et al.*, Opt. Lett. **29**, 286 (2004).
[26] S. López-Aguayo *et al.*, Opt. Express **14**, 7903 (2006).
[27] O. Bang *et al.*, Phys. Rev. E **66**, 046619 (2002).
[28] M. Peccianti *et al.*, Opt. Lett. **27**, 1460 (2002).
[29] M.-F. Shih, M. Segev, and G. Salamo, Phys. Rev. Lett. **78**, 2551 (1997).
[30] P. Pedri and L. Santos, Phys. Rev. Lett. **95**, 200404 (2005); R. Nath, P. Pedri, and L. Santos, Phys. Rev. A **76**, 013606 (2007).
[31] H. Saito and M. Ueda, Phys. Rev. Lett. **90**, 040403 (2003); A. M. Kamchatnov and L. P. Pitaevskii, Phys. Rev. Lett. **100**, 160402 (2008).
[32] S. Giovanazzi, A. Görlitz, and T. Pfau, Phys. Rev. Lett. **89**, 130401 (2002).
[33] D. N. Christodoulides and R. I. Joseph, Opt. Lett. **13**, 794 (1988); A. Trombettoni and A. Smerzi, Phys. Rev. Lett. **86**, 2353 (2001).
[34] M. Krämer *et al.*, Phys. Rev. Lett. **88**, 180404 (2002).
[35] $C \simeq \sum_{i\neq 0, j\neq 0} |\tilde{n}(2\pi i/b, 2\pi j/b)|^2$ where $\tilde{n}$ is the Fourier transform of n and $n(x, y) = |w(x, y)|^2$.
[36] M. Klawunn *et al.*, Phys. Rev. Lett. **100**, 240403 (2008).
[37] The lattice-induced large-momentum cutoff is introduced in our simulations of Eq. (2) by the numerical grid in the xy-plane.
[38] J. Dziarmaga and K. Sacha, Phys. Rev. A **66**, 043615 (2002).